AIAA 80-0997R

Propeller Light Aircraft Noise at Discrete Frequencies

Claude Dahan,* Léon Avezard,† Georges Guillien,‡
Christian Malarmey,§ and Jacques Chombard¶
Office National d'Etudes et de Recherches Aérospatiales, Châtillon, France

In-flight measurements are analyzed to study the acoustic field of a propeller-driven light aircraft. The separation of noise sources is achieved by examination of the influence on the acoustic field of the propeller and the engine. At high rotational speed, the propeller is the dominant source. Evaluating then the field due to steady/unsteady loading on the blades, one concludes that the former are acoustically the most efficient. The analysis of flyover noise measurements, using an original signal processing (Doppler effect compensation) enhances the results.

Nomenclature

$a(r)$ = blade transversal section
B = number of blades
c = velocity of sound
$\mathcal{C}(f)$ = normalized cross spectrum
$\mathcal{C}_l(f)$ = coherency function
D = force component in the propeller plane
F_L = loads components
$F(r)$ = loads spanwise distribution function
$f_{mB}(r)$ = loads chordwise distribution function
f = frequency
G = Green's function
h = height of a microphone above the ground
$J_m(z)$ = Bessel function of order m
k = wave number $= 2\pi f/c$
M = advancing Mach number
pe = acoustic pressure due to thickness
$(pe)_m$ = mth Fourier component of pe
p_l = acoustic pressure due to loads
$(p_l)_m$ = mth Fourier component of p_l
p_d = direct pressure
p_r = reflected pressure
$Q(r)$ = element of torque
r = spanwise coordinate
R_0 = radius at the boss
R_l = radius of the propeller
S = modified distance
$T(r)$ = element of thrust
T_{ij} = Lighthill tensor
$t, \hat{t}$ = time
V = advancing velocity
W = aircraft's weight
(x,y,z) = observer's coordinates
D/Dt = material derivative
α = ground reflection angle
β = Doppler factor ($\beta^2 = 1 - M^2$)
δ = phase angle
Γ = vortex circulation
$\Delta(f)$ = phase angle
ψ = azimuthal angle
ρ_0 = air density
τ = time
η = propeller's efficiency
Ω = rotational velocity

Presented as Paper 80-0997 at the AIAA 6th Aeroacoustics Conference, Hartford, Conn., June 4-6, 1980; submitted July 23, 1980; revision received March 11, 1981.

*Research Engineer.
†Electronics Engineer.
‡Acoustics Technician.
§Acoustics Technician.
¶Electronics Technician.

I. Introduction

WHEN studying the noise field radiated by light propeller-driven aircraft, a first task is the identification of the noise sources. In this work, we are concerned with the piston-engine aircraft of the 180-235 hp class. For the discrete tones emitted by these aircraft, it is usual to distinguish as noise sources, on one hand, the propeller and, on the other, the engine and its exhaust pipe. The assessment of these two important components is then needed. Thus, a method allowing this noise source separation is outlined.

Turning then to the acoustic efficiency of the propeller, our aim is to emphasize the relevant parameters for this radiation (influence of steady loads on the propeller disk, of blade thickness, of unsteady loads due to propeller-fuselage interactions), which is done using some computer codes we will describe. The results of these acoustic prediction schemes are then compared to experimental data provided by in-flight measurements.

Finally, considering that in-flight measurements explore only a limited area, the experiment is completed by flyover measurements, using a ground-fixed microphone and a signal processing analysis.

II. Noise Source Separation

Two types of aircraft were considered, 235 and 180 hp Rallyes. For the former, the separation is obvious: this aircraft is commonly equipped with a six-cylinder engine and a two-bladed propeller, so that the characteristic frequencies of these two components generally do not overlap. This is illustrated in Fig. 1, which represents an acoustic power spectral density measured in flight (see Sec. IIB). For the 180 hp Rallye, equipped with a four-cylinder engine and a two-bladed propeller, the characteristic frequencies overlap and the noise source separation becomes difficult.

A. Static Tests

A measure of the acoustic field of the engine only is first tried in static tests. The engine is mounted on a test stand; its power is absorbed by a Froude brake. These measurements give an estimation of the acoustic efficiency of this engine (Fig. 2). Nevertheless, they must be taken cautiously because, without the propeller, the engine lacks cooling and the allowed time to measure the acoustic pressure is short. Thus, precise in-flight measurements must be made to confirm that the propeller is the dominant noise source (Fig. 2).

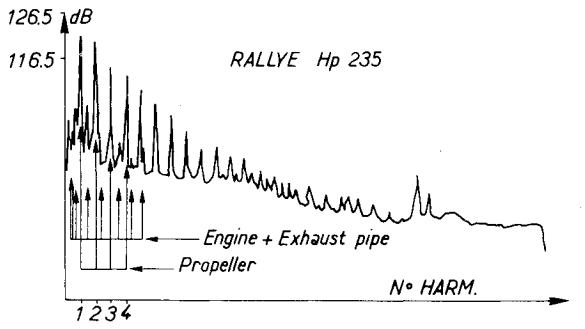

Fig. 1 Power spectral density micro $a-N=2550$ tr/mn.

B. In-Flight Measurements

Six microphones were set under the wings at a distance between 60 and 80 cm from the leading edge. A photoelectric cell giving a square signal when the blades are vertical allows the synchronization of the acoustic measurements and the propeller rotation. Moreover, the frequencies are too low to permit the use of phase differences between microphones to determine a source location; however, the position of the propeller on the engine shaft (six bolts) allows one to modify the relative setup of the propeller and the engine in the following way:

If T is the time for a cycle of the engine, the period is $T/2$, and the blade passing frequency $T/4$. Turning the propeller by $\pi/3$ around its axis (the engine position being fixed) translates in time the signal coming from the engine by an amount $T/6$. We can then write the following equalities.

First flight (standard setup):

$S(t)$	$=$	$S_0(t)$	$+$	$S_1(t)$
Acoustic signal on any microphone		Propeller contribution		Engine + exhaust contribution

Second flight (modified setup):

$$S'(t)=S_0(t)+S_1(t-T/6)$$

In the frequency domain (f standing for the frequency)

$$S(f)=S_0(f)+S_1(f)$$

$$S'(f)=S_0(f)+S_1(f)e^{-2i\pi fT/6}$$

For a blade passing frequency harmonic

$$f=4n/T$$

$$S'(f)=S_0(f)+S_1(f)e^{-2in\pi/3}$$

Theoretically, these two equations already determine the power spectral densities of the propeller ($|S_0(f)|^2$) and the engine ($|S_1(f)|^2$). Nevertheless, taking into account the problems linked to such a method (from one flight to another the signals are not very stable, etc.), we were led to use some concepts from broadband noise theory, giving then the normalized cross spectrum between S and S'

$$\mathcal{C}(f)=\frac{\langle S(f)S^{*\prime}(f)\rangle}{\langle S^2(f)\rangle^{1/2}\langle S'^2(f)\rangle^{1/2}}$$

The brackets indicate an ensemble average over several periods:

1) The function $\mathcal{C}_1(f)=|\mathcal{C}(f)|$ is the coherency between S and S' at the frequency f. If $\mathcal{C}_1(f)=1$ the corresponding spectral line is stable.

2) The function $\Delta\Phi(f)=$ phase of $\mathcal{C}(f)$ is the relative phase of S and S' (the phase origin being fixed by the photocell).

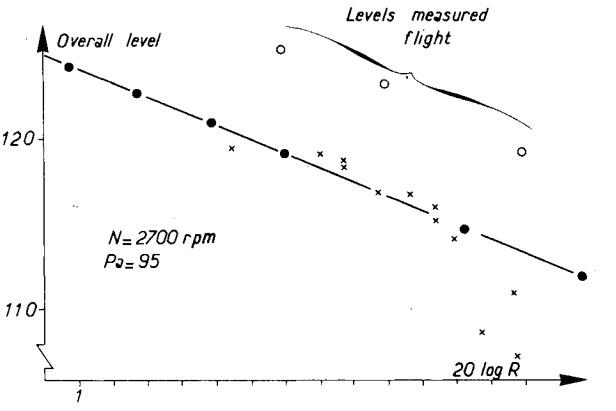

Fig. 2 Evolution of the overall level with the distance to the engine.

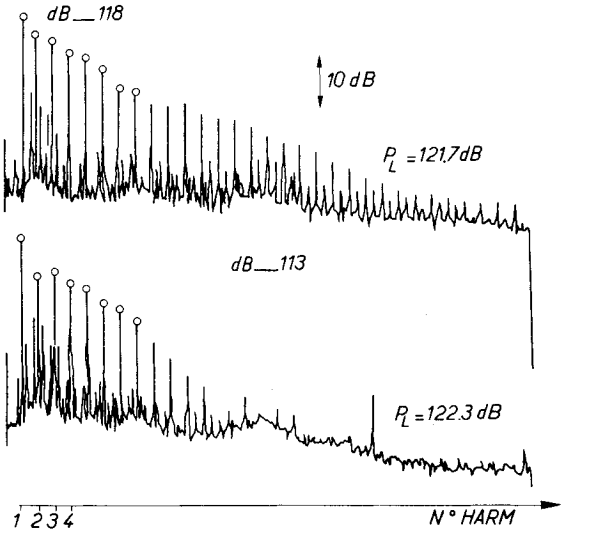

Fig. 3 Power spectral densities of a microphone measured during two successive flights.

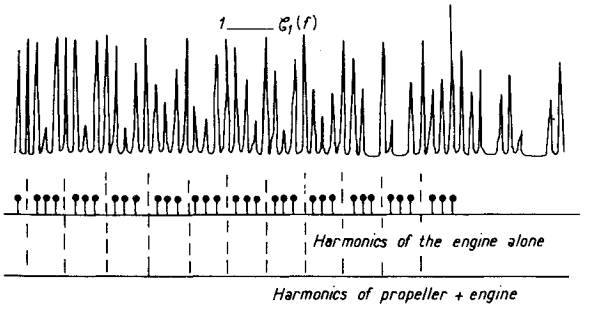

Fig. 4 Coherency function between microphone's signals measured in two successive flights.

If $\Delta\Phi(f)\approx 0$, the spectral line corresponding to the frequency f may be attributed to the propeller. If $\Delta\Phi(f)=2\pi fT/6=2n\pi/3$, the spectral line is due to the engine.

The noise power spectral densities measured during two successive flights are quite similar (Fig. 3): the coherency $\mathcal{C}_1(f)$ is close to 1 for the main spectral lines (Fig. 4), and the relative phases $\Delta\Phi(f)$ are near 0 (Fig. 5). Thus the radiated acoustic intensity is essentially attributed to the propeller. These results are unambiguous at high rotational velocities ($\geq$2400 rpm), but it seems that for lower regimes ($<$2400 rpm), the engine becomes an important noise source.

With the predominance of the propeller with respect to noise emission thus established, the mechanism responsible for this noise emission is now considered.

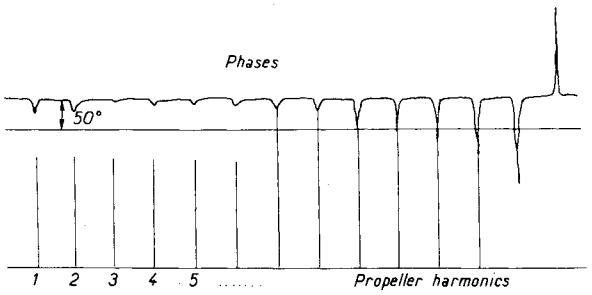

Fig. 5 Relative phase of microphone's signal measured in two successive flights.

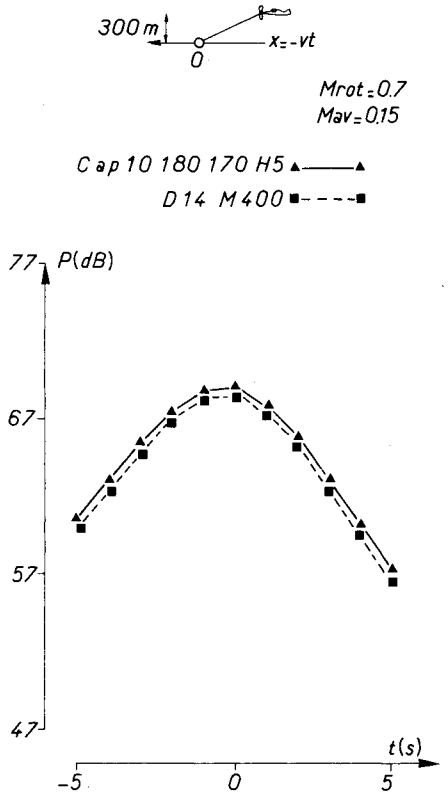

Fig. 6 Directivity pattern for the thickness noise.

III. Propeller Noise

The prediction schemes described are derived from the Lighthill analogy, modified by Goldstein[1] to account for the aircraft motion, and give the acoustic pressure in the following integral form

$$p=\int_A \rho_0 V_n' \frac{DG}{D\tau}\mathrm{d}\vec{y}+\int_A F_i \frac{\partial G}{\partial y_i}\mathrm{d}\vec{y}+\int_V T_{ij}\frac{\partial^2 G}{\partial y_i \partial y_j}\mathrm{d}\vec{y}$$

As usual: the first integral, linked to the air volume displaced by the blades, is the thickness noise term; the second one, associated to the forces on the blades accelerating the surrounding fluid, is the loading term; and the third takes into account the stresses in the flow around the blades (quadrupolar noise). Only the first two quantities, quite important for subsonic propellers, are retained.

A. The Thickness Noise

Developing the quantity

$$\int_A \rho_0 V_n' \frac{DG}{D\tau}\mathrm{d}\vec{y}$$

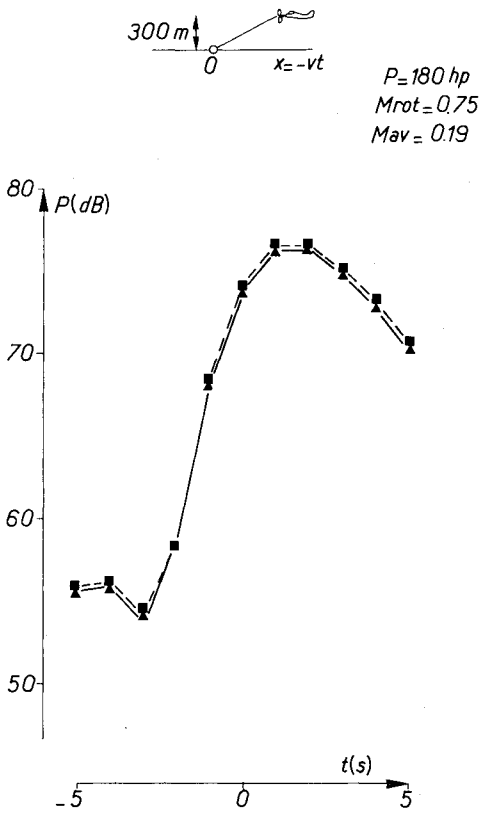

Fig. 7 Influence of the chordwise loads distribution on the radiated field chordwise loads distribution. ■ $\sin(mBb\cos\theta_b/2r)2r/mBb\cos\theta_b$; ▲ $J_0(mBb\cos\theta_b/2r)-iJ_1(mBb\cos\times\theta_b/2r)$.

specifically for a propeller (Fig. 6) gives:

$$(pe)_m=-\frac{\rho_0 Bk^2c^2}{4\pi\beta^4 S}\left(1+\frac{Mx}{S}\right)^2 e^{imB(\varphi+\pi/2)}$$

$$\times e^{-(ik/\beta^2)(Mx+S)}\int_{R_0}^{R_1} a(r)J_{mB}(kAr)\,\mathrm{d}r$$

This is the formula given by Arnoldi,[2] slightly modified to include the velocity of the propagative medium.

p_m stands for the Fourier coefficient, for the mth harmonic of the blade passing frequency. The quantities A and φ are defined by

$$A\cos\varphi=y/S \qquad A\sin\varphi=-z/S$$

where S is a distance modified by the amplitude Doppler effect

$$S=[x^2+\beta^2(y^2+z^2)]^{1/2}$$

A numerical application of this formula for a two-bladed propeller is shown in Fig. 6. One can see that the radiated field has a principal lobe directed slightly upward to the propeller plane.

B. Loading Noise

Two types of mechanisms are distinguished: 1) the noise due to steady loads on the blades (most of the theoretical results concerning this source mechanism were obtained a long time ago by Gutin[3] and Garrick and Watkins[4]); and 2) the noise due to unsteady loads.

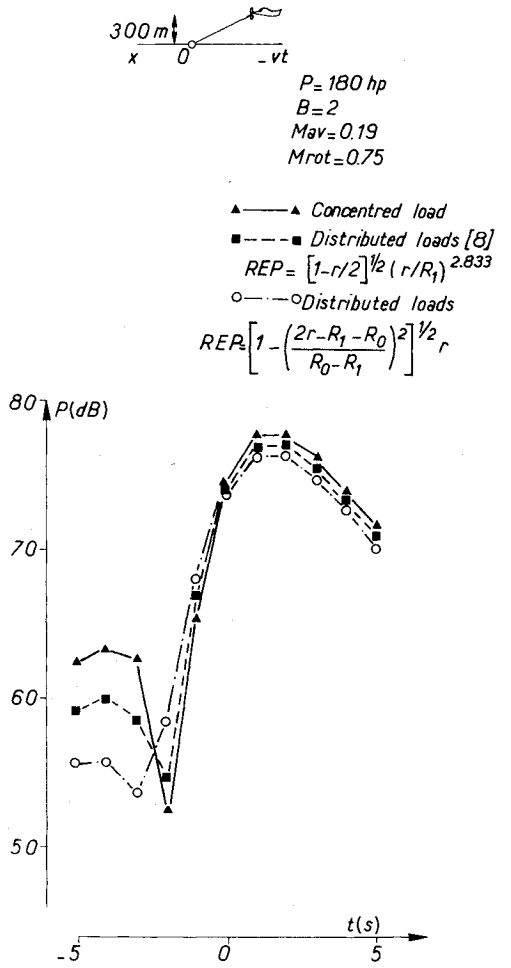

Fig. 8 Influence of spanwise loads distribution.

An analytical formulation of the steady loading term is written

$$(p_L)_m = \frac{iBk}{4\pi S} e^{imB\varphi} e^{-(ik/\beta^2)(Mx+S)} \int_{R_0}^{R_1} \left[\left(M + \frac{x}{S} \right) \frac{T(r)}{\beta^2} - \frac{mBQ(r)}{kr^2} \right] f_{mB}(r) J_{mB}(kAr)\, dr$$

where $T(r)$ and $Q(r)$ represent thrust and torque element at the span r and $f_{mB}(r)$ describes the chordwise distribution of the loads, and essentially depends on the propeller disk solidity, always weak in these cases, so that $f_{mB}(r) \approx 1$ (Fig. 7). The comparison between concentrated forces, uniform chordwise distribution of loads, and the plane plate distribution[5] shows the slight importance of the precise form $f_{mB}(r)$ in the acoustic prediction scheme. Concerning the spanwise distribution $T(r)$ and $Q(r)$, the elementary following equations are considered. If P is the available power on the engine shaft, the total thrust and torque are given by

$$\eta P = TV \qquad P = \Omega Q$$

In steady, horizontal flight, the propeller efficiency η is generally high, and in these computations is assumed to be 1. Now, we can introduce a spanwise distribution function $F(r)$ such that:

$$T(r) = TF(r) \qquad Q(r) = QF(r); \qquad \int_{R_0}^{R_1} F(r)\, dr = 1$$

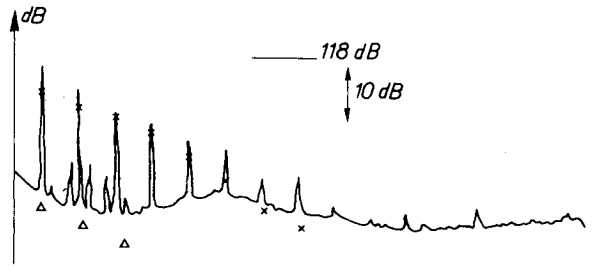

Fig. 9 Influence of wing effects on the radiated noise. × steady loads + thickness (theory); Δ unsteady loads (wing effect); V. P. propeller Hartzell; $N = 2650$ rpm; $V = 225$ km/h.

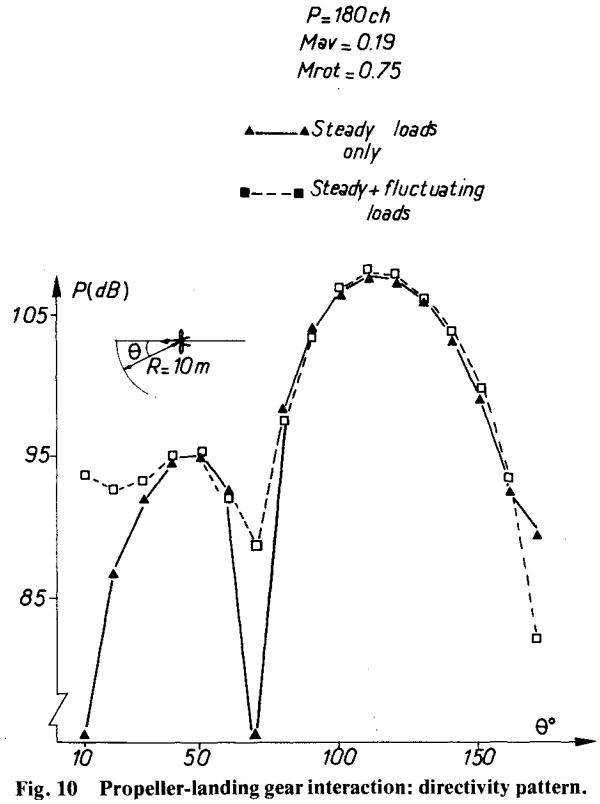

Fig. 10 Propeller-landing gear interaction: directivity pattern.

A reasonable function for $F(r)$ could be:

$$F(r) = C^{te} r \left[1 - \left(\frac{2r - R_1 - R_0}{R_1 - R_0} \right)^2 \right]^{1/2}$$

where the square root is due to the finite length of the blades, and the multiplication by the spanwise coordinate r to the spanwise increasing efficiency of blade elements.[6] Once more, one can see that the precise form of the function $F(r)$ is not critical (Fig. 8).

Considering now the noise generated by the unsteady loads, a generalization of a Goldstein formula to the advancing flight situation leads to

$$(p_L)_m = \frac{iBk}{4\pi S} \sum_{s=-\infty}^{+\infty} e^{i(mB-s)(\varphi-\pi/2)} \times \int_{R_0}^{R_1} \left[\left(M + \frac{x}{S} \right) \frac{T(r,s)}{\beta^2} - \frac{(mB-s)}{kr} Q(r,s) \right] \times f_{mB-s}(r) J_{mB-s}(kAr)\, dr$$

When $s = 0$, one again gets the pressure field due to steady loads.

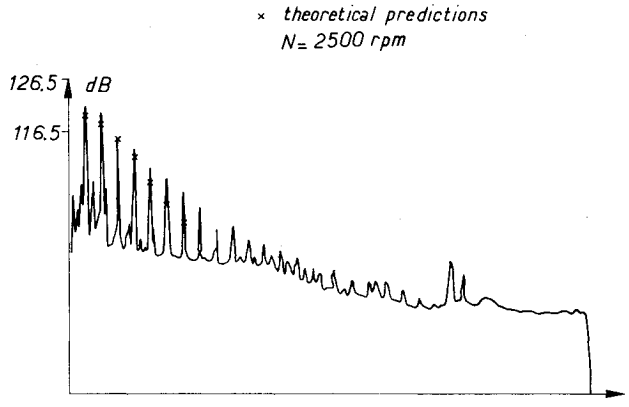

Fig. 11 Comparison of measured and predicted levels (in-flight measurements).

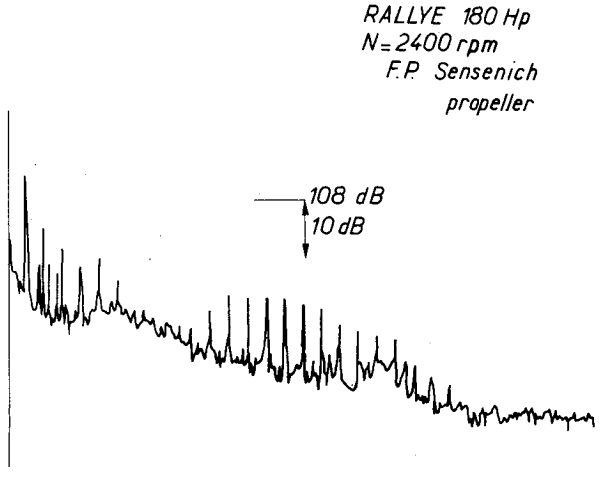

Fig. 12 Apparition of a propeller's higher order harmonics bunch.

To use such a formulation, the knowledge of the fluctuating loads $T(r,s)$ and $D(r,s)$, that is, of the propeller-fuselage interactions is needed. Two elements then arise: the propeller-wing interactions and the propeller-landing gear interactions.

Propeller Wing Interactions

The mechanism of this interaction is described in Ref. 5: the wing represents a lifting surface that creates an upwash velocity u in the propeller plane. The representation of the wing by a bounded vortex of constant circulation Γ, which is estimated from the aircraft weight W

$$W=\rho_0 \Gamma V$$

allows one to calculate the upwash u

$$u=\Gamma/2\pi r$$

The expression for the flight derivatives given by Glauert[6] can here be used

$$\delta T=\frac{2u\cos\psi}{\Omega r}\left[T-\tfrac{1}{2}\Lambda\frac{\partial T}{\partial \Lambda}\right]$$

$$\delta D=\frac{2u\sin\psi}{\Omega r}\left[D-\tfrac{1}{2}\Lambda\frac{\partial D}{\partial \Lambda}\right]$$

where Λ stands for the advance ratio $V/\Omega R_l$.

To use these formulas, the characteristics $T(\Lambda)$ and $D(\Lambda)$ must be known, which is difficult because of the lack of lift and drag curves for the airfoils representative of the blade

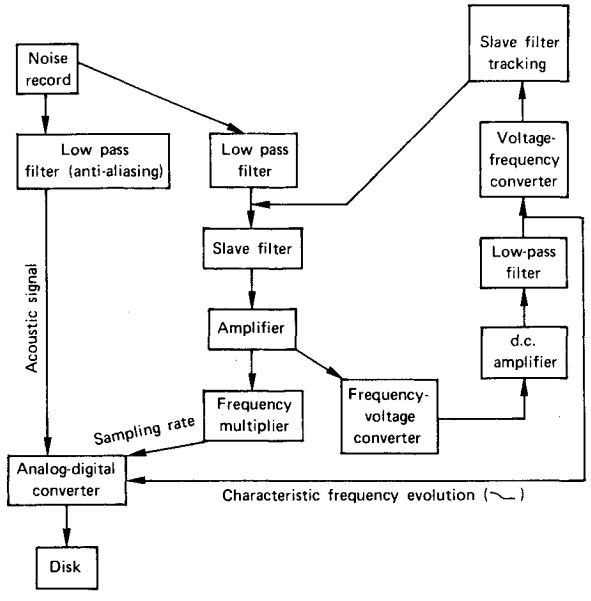

Fig. 13 Arrangement to build up an adapted sampling rate for the acoustic signal and to follow the aircraft during its motion.

sections. Thus these curves are crudely estimated to fit correctly the propeller performances measured in flight. As shown in Fig. 9, the effect of wing-propeller interaction is slight.

Propeller-Landing Gear Interactions

Because the landing gear is downstream of the propeller plane, a "potential" interaction exists. This kind of interaction was emphasized by SNIAS in describing the acoustic field generated by helicopter rear rotors of the "Fenestron" type.[7]

When introducing force fluctuations in the acoustic prediction scheme, it appears that the interaction effects is strongest for the harmonics of order $m\approx 3.4$, but that it remains quite below the effect of steady loads. The acoustic intensity directivity pattern shows that the effect of this kind of unsteady loading is to fill up the holes in the diagram associated with steady loadings (Fig. 10).

C. Comparison with In-Flight Measurements

Retaining only the thickness and steady loads terms in the acoustic field computation, predictions and measurements agree reasonably well, especially for the microphones located at the tips of the wings (Fig. 11). Nevertheless, some facts remain unexplained:

1) The field is not completely symmetrical with regard to the aircraft axis: the acoustic pressure on the left wing is higher than that on the right wing.

2) For some operating conditions (rotational speed <2400 rpm), a bunch of higher order harmonics can appear (Fig. 12), but it is not very stable (it can disappear for another flight at the same operating conditions). This kind of spectral shape was also noted elsewhere, in the analysis of flyover measurements.[8]

IV. Flyover Analysis

A. Signal Processing

The flyover analysis is to verify assumptions made concerning the mechanisms responsible for the propeller noise emission. However, we do not want to go into the complexity of coupling the acoustic signal with optical information coming from, for instance, ciné-théodolites. The difficulty of this last procedure can be avoided by taking advantage of the fact that, in given flight conditions, a characteristic tone of the aircraft will be perceived as time evoluting, and that the

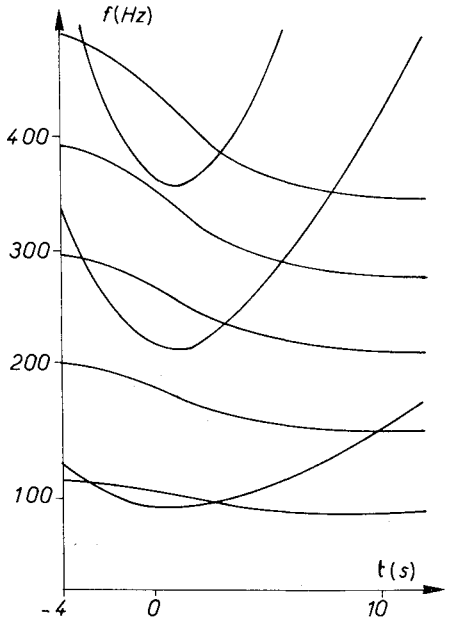

Fig. 14 Simultaneous evolution of the perceived frequency (Doppler effect) and of the extinction frequency f_c.

Fig. 15 Time evolution of a propeller's tone during a flyover.

detection of this frequency evolution is equivalent to following the aircraft motion. The signal processing method derived from these considerations is described in Ref. 9, where it was applied to the analysis of helicopter flyovers.

An adapted sampling rate compensates the Doppler effect due to the advancing motion of the aircraft, so that a specified elementary filter in the Fourier analysis will correspond to a fixed tone generated by the aircraft. Three operations are then necessary (see Fig. 13): detection of a source characteristic frequency (evolutive frequency), synchronization of the sampling rate for the detected frequency, and Fourier analysis driven by the previous sampling rate.

This basic scheme is complicated slightly by the fact that an acoustic signal obtained under certification conditions, with a microphone at a height $h = 1.2$ m above the ground, must be analyzed including the ground reflection phenomena. For this, we can follow Ref. 3.

The total field at the microphone is expressed as the sum of the direct and reflected pressure waves:

$$p = p_d + p_r = p_d [1 + Re^{i\delta}]$$

where R stands for a ground reflection coefficient, δ the phase difference between p_d and p_r depends on the retarded time $\hat{t}$ via the perceived frequency f and the incidence angle $\alpha(\hat{t})$:

$$\delta = \frac{4\pi f h \sin\alpha(\hat{t})}{c}$$

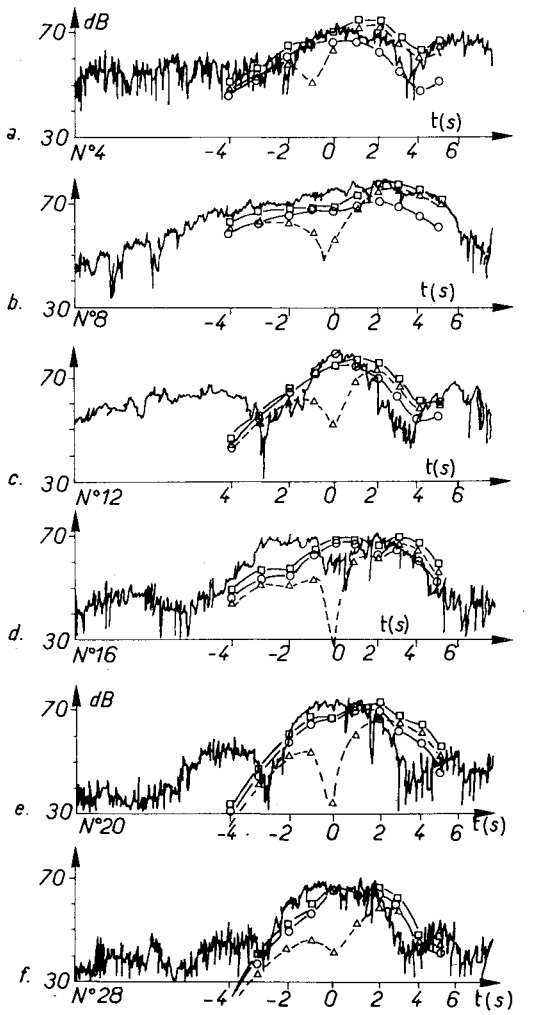

Fig. 16 Harmonic levels evolution during the flyover.——○ thickness; - - - - △ loads (theory); —— □ total.

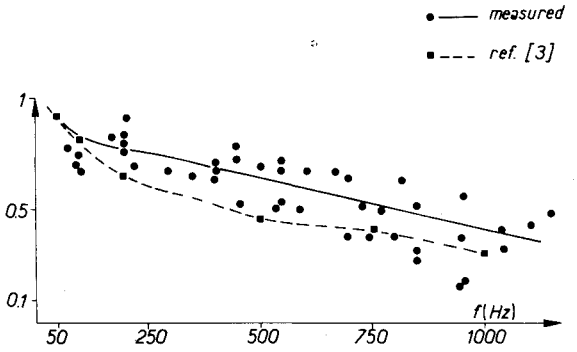

Fig. 17 Ground reflection coefficient.

For some values of f, there is an almost perfect cancellation of the signal $[\delta = (2n+1)\pi]$.

These values are given by:

$$f_c = (2n+1)c/4h\sin\alpha(\hat{t})$$

The simultaneous evolution of f_c and of the characteristic tones of the propeller is drawn on Fig. 14 and shows that the signal cancellations prevent the slave filter from operating correctly. This can be avoided when the detection setup is in a loop (Fig. 13). Then, the flight of the aircraft is followed (Fig. 15), an adapted sampling rate is built up, and we get directly the evolution of any harmonic of the blade passing frequency (Fig. 16).

B. Comparison with Theoretical Predictions

An estimation of the ground reflection coefficient R (Sec. IVA) must be introduced. This is done[3] by comparison, on instantaneous power spectral densities, of the amplitudes in a hole due to reflection and between two holes:

$$\frac{|p(2nf_c)|^2}{|p[(2n+1)f_c]|^2} = \frac{(1+R)^2}{(1-R)^2}$$

As, for low frequencies, those instantaneous spectra are essentially made of discrete tones. The estimations of R are rather scattered, but nevertheless show a trend (Fig. 17).

Correcting thus the free-field estimations (Sec. II) by the ground reflection term (Sec. IVA), the predictions are recast in a form directly comparable to the experimental data provided by our flyover analysis (Fig. 16). The importance of the blade thickness mechanism before the overhead point and the dominance of the loading term after this point are shown. Nevertheless, the predictions are not accurate when the aircraft approaches the overhead position.

V. Conclusion

The first objective was to assess the relative importance of the two major acoustic sources for light, propeller-driven aircraft, namely the engine and the propeller. A method to analyze the noise field measured in flight was developed which shows that the propeller is the dominant noise source for high rotational speeds.

The evaluation of the mechanisms responsible for the propeller noise emission shows that, for these high operating tip Mach numbers ($M \sim 0.8$), the unsteady loads arising from blade-fuselage interactions (wings and landing gear) do not contribute much to the acoustic field, essentially due to steady loads and to the fluid volume displaced by the blades during their motion. A better knowledge of the aerodynamic behavior of the propeller is needed (correct prediction of its efficiency). In the same way, to confirm our conclusions concerning the acoustic efficiency of unsteady loads, direct measurements of the blade fluctuating pressure would be very helpful. Nevertheless, predictions compared to in-flight measurements show agreement. For completeness, flyover noise analyses were made, using a signal processing method tailored to compensate for the Doppler effect due to the aircraft advancing motion. They point out the importance of the blade thickness upstream of the propeller disk and of the blade loads downstream. A better account of ground reflection phenomenon is needed to refine these conclusions.

References

[1] Goldstein, M. V., "Aeroacoustics," NASA SP-346, 1974.

[2] Arnoldi, A., "Thickness Noise of Propellers," NACA TN 08091-1, 08096-2, 1958.

[3] Gutin, L., "On the Sound Field of a Rotating Propeller," NACA TM 1195, Oct. 1948.

[4] Garrick, I. E. and Watkins, C. E., "A Theoretical Study of the Effect of Forward Flight on the Free Space Sound Pressure Field around Propellers," NACA Rept. 1198, 1954.

[5] Griffith, J. D. and Revell, E. D., "Low Noise Propeller Technology," AFAPL TR-73-115, Dec. 1973.

[6] Glauert, H., "Airplane Propellers," *Aerodynamic Theory*, Durand, Dover, 1963.

[7] D'Ambra, F. and Damangeot, A., "Noise Generation by Potential Flow Interaction of Fans and Shrouded Propellers," Communication presented at Gart-Eur 5 meeting, Paris, 1977.

[8] Heller, H. H. et al., "Rotational and "Vortex" Noise of Propellers in the 100 to 150 kW Class," AIAA Paper 79-0611, 1979.

[9] Dahan, C. and Gratieux, E., "Helicopter Thickness Noise," AIAA Paper 80-1017, 1980.